RESEARCH ARTICLE

Nonribosomal Peptides, Key Biocontrol Components for *Pseudomonas fluorescens* In5, Isolated from a Greenlandic Suppressive Soil

Charlotte F. Michelsen,[a]* Jeramie Watrous,[b,c,d] Mikkel A. Glaring,[a] Roland Kersten,[b,c,d] Nobuhiro Koyama,[e] Pieter C. Dorrestein,[b,c,d] Peter Stougaard[a]

Department of Plant and Environmental Sciences, University of Copenhagen, Copenhagen, Denmark[a]; Department of Pharmacology, University of California at San Diego, La Jolla, California, USA[b]; Department of Chemistry and Biochemistry, University of California at San Diego, La Jolla, California, USA[c]; Skaggs School of Pharmacy and Pharmaceutical Sciences, University of California at San Diego, La Jolla, California, USA[d]; Graduate School of Pharmaceutical Sciences, Kitasato University, Tokyo, Japan[e]

* Present address: Charlotte F. Michelsen, Department of Systems Biology, Technical University of Denmark, Kongens Lyngby, Denmark.

ABSTRACT **Potatoes are cultivated in southwest Greenland without the use of pesticides and with limited crop rotation. Despite the fact that plant-pathogenic fungi are present, no severe-disease outbreaks have yet been observed. In this report, we document that a potato soil at Inneruulalik in southern Greenland is suppressive against *Rhizoctonia solani* Ag3 and uncover the suppressive antifungal mechanism of a highly potent biocontrol bacterium, *Pseudomonas fluorescens* In5, isolated from the suppressive potato soil. A combination of molecular genetics, genomics, and matrix-assisted laser desorption ionization–time of flight (MALDI-TOF) imaging mass spectrometry (IMS) revealed an antifungal genomic island in *P. fluorescens* In5 encoding two nonribosomal peptides, nunamycin and nunapeptin, which are key components for the biocontrol activity by strain In5 *in vitro* and in soil microcosm experiments. Furthermore, complex microbial behaviors were highlighted. Whereas nunamycin was demonstrated to inhibit the mycelial growth of *R. solani* Ag3, but not that of *Pythium aphanidermatum*, nunapeptin instead inhibited *P. aphanidermatum* but not *R. solani* Ag3. Moreover, the synthesis of nunamycin by *P. fluorescens* In5 was inhibited in the presence of *P. aphanidermatum*. Further characterization of the two peptides revealed nunamycin to be a monochlorinated 9-amino-acid cyclic lipopeptide with similarity to members of the syringomycin group, whereas nunapeptin was a 22-amino-acid cyclic lipopeptide with similarity to corpeptin and syringopeptin.**

IMPORTANCE **Crop rotation and systematic pest management are used to only a limited extent in Greenlandic potato farming. Nonetheless, although plant-pathogenic fungi are present in the soil, the farmers do not experience major plant disease outbreaks. Here, we show that a Greenlandic potato soil is suppressive against *Rhizoctonia solani*, and we unravel the key biocontrol components for *Pseudomonas fluorescens* In5, one of the potent biocontrol bacteria isolated from this Greenlandic suppressive soil. Using a combination of molecular genetics, genomics, and microbial imaging mass spectrometry, we show that two cyclic lipopeptides, nunamycin and nunapeptin, are important for the biocontrol activity of *P. fluorescens* In5 both *in vitro* and in microcosm assays. Furthermore, we demonstrate that the synthesis of nunamycin is repressed by the oomycete *Pythium aphanidermatum*. Overall, our report provides important insight into interkingdom interference between bacteria and fungi/oomycetes.**

Received 15 January 2015 **Accepted** 11 February 2015 **Published** 17 March 2015

Citation Michelsen CF, Watrous J, Glaring MA, Kersten R, Koyama N, Dorrestein PC, Stougaard P. 2015. Nonribosomal peptides, key biocontrol components for *Pseudomonas fluorescens* In5, isolated from a Greenlandic suppressive soil. mBio 6(2):e00079-15. doi:10.1128/mBio.00079-15.

Editor E. Peter Greenberg, University of Washington

Address correspondence to Peter Stougaard (queries on microbial genetics work), psg@plen.ku.dk, or Pieter C. Dorrestein (queries on imaging MS), pdorrestein@ucsd.edu.

Agriculture in subarctic Greenland is possible without pesticides and with limited crop rotation despite the presence of plant-pathogenic fungi. For example, potatoes cultivated in a small single field at the Agricultural Consulting Services in Qaqortoq for almost 50 years showed no severe incidence of diseases such as potato late blight (K. Høegh, personal communication). One plausible explanation is that these Greenlandic soils are disease suppressive, i.e., they contain beneficial microbes that positively affect the growth and health of plants (1, 2). Suppressive soils have been described from several parts of the world, including *Fusarium* wilt-suppressive soils from Chateaurenard (France) and the Salinas Valley (United States), potato scab-suppressive soils from Washington (United States), and suppressive sugar beet soils (the Netherlands) (2, 3). Beneficial microorganisms responsible for suppression of fungal growth, the so-called biological control agents (BCAs), have been discovered among bacteria of several genera, e.g., *Bacillus*, *Alcaligenes*, *Burkholderia*, *Agrobacterium*, and *Pseudomonas* (1–4). Of these, fluorescent pseudomonads have been investigated in the greatest detail, and antifungal compounds, including phenazines, pyoluteorin, phloroglucinols, pyrrolnitrin, hydrogen cyanide (HCN), and nonribosomal peptides (NRPs), have been identified (5).

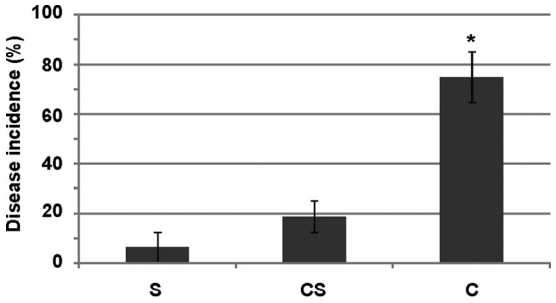

FIG 1 Soil microcosm experiment. Presprouted tomato seedlings were planted in the Inneruulalik suppressive soil (S), in the Inneruulalik soil heat treated at 80°C (C, conducive), and in heat-treated soil mixed with the suppressive soil (9:1 [wt/wt]) (CS). Damping-off symptoms of infected seedlings caused by *R. solani* Ag3 were scored visually and expressed as percentages of disease incidence (means ± standard errors of the means [SEM], $n = 4$). The asterisk indicates a statistically significant difference from the suppressive soil (S) ($P < 0.05$, Tukey's HSD test).

A *Pseudomonas* strain with high antifungal activity was previously isolated from a potato field at Inneruulalik, southern Greenland (6). This bacterium, *Pseudomonas fluorescens* In5, inhibited a wide range of pathogenic fungi and oomycetes *in vitro* in a temperature-dependent manner, i.e., showing higher activities at lower temperatures (6). Previous attempts to identify antifungal compounds such as phenazines, pyoluteorin, phloroglucinols, and pyrrolnitrin, or the genes encoding such compounds in *P. fluorescens* In5, were unsuccessful. The only putative antifungal compound identified was HCN, but genetic analysis indicated that an unknown NRP might also be involved in the antifungal activity of this strain (6, 7). The actual NRP, however, was never identified or isolated.

In this study, we unraveled the antifungal mechanism of the disease-suppressive *P. fluorescens* In5 strain using a combination of *in vitro* agar plate assays, soil microcosm experiments, molecular genetics, genomics, and matrix-assisted laser desorption ionization–time of flight (MALDI-TOF) imaging mass spectrometry (IMS) analyses. We show that the main biocontrol ability of *P. fluorescens* In5 is mediated by two lipopeptides with distinct fungal inhibition activities depending on the target fungus or oomycete.

RESULTS

Potato soil from Inneruulalik in southern Greenland is disease suppressive. Soil samples were collected from a potato field at Inneruulalik in southern Greenland. According to the farmer, potatoes were cultivated in the same plot for at least 10 consecutive years without any incidence of severe diseases. The disease-suppressive properties of the soil were investigated using *in vitro* soil microcosm experiments with seedlings of tomato (a member of the same plant family as potatoes, *Solanaceae*) and the plant-pathogenic basidiomycete *Rhizoctonia solani* Ag3 causing, e.g., stem rot and tuber black scurf of potatoes. Seedlings planted into the Inneruulalik soil inoculated with *R. solani* Ag3 mycelium did not show any damping-off symptoms, whereas a heat treatment of the soil (80°C for 1 h), followed by *R. solani* Ag3 inoculation, led to severely affected seedlings (Fig. 1). In addition, the disease-suppressive properties of the heat-treated soil could be almost completely recovered by mixing in a small (10%) amount of the untreated soil (Fig. 1), which suggests that the Inneruulalik soil is suppressive against *R. solani* Ag3 and that the suppressive mechanism is of microbiological origin. Metagenomic DNA was isolated from the Inneruulalik suppressive soil, and pyrosequencing generated a total of 30,747 high-quality sequences revealing members of the phyla *Proteobacteria*, *Bacteroidetes*, *Actinobacteria*, and *Acidobacteria* to be the most abundant bacteria in the soil microbiome (see Table S1 in the supplemental material). Members of the bacterial genera *Pseudomonas*, *Bacillus*, *Paenibacillus*, *Streptomyces*, and *Burkholderia* have previously been described for their biocontrol activities (8–11); however, the culture-independent pyrosequencing analysis showed that these bacterial genera constituted only a small fraction of the total diversity in the Inneruulalik soil (see Table S2). Previously, a potent antifungal pseudomonad, *P. fluorescens* In5, was identified from the Inneruulalik potato soil using culture-based approaches (6); hence, this biocontrol bacterium was the subject of the subsequent studies.

Molecular genetics of *P. fluorescens* In5 reveal an antifungal genomic island encoding nonribosomal peptides with distinct antifungal activities. To identify genes in *P. fluorescens* In5 encoding antifungal compounds, a Tn*5* transposon mutant library was constructed and the approximately 1,500 mutants were arranged in microtiter plate format and screened for loss of mycelial growth inhibition of *R. solani* Ag3 or *Pythium aphanidermatum* (an oomycete causing leak syndrome of potatoes) *in vitro*. One mutant, Tn1, failed to inhibit mycelial growth of *R. solani* Ag3, whereas inhibition of *P. aphanidermatum* was slightly increased compared to the level seen with wild-type strain In5 (Fig. 2A; see also Fig. S1 in the supplemental material). DNA sequence analysis of the insertion site showed that the transposon had inserted into an open reading frame (ORF), *nunE*, encoding a putative NRP (Fig. 3). Interestingly, a closer examination of the whole-genome sequence of *P. fluorescens* In5 revealed that the genomic region around the transposon insertion site contained a number of ORFs with similarities to known NRP genes from *P. syringae* pv. *syringae* B728a, Cit7, and 642 and from *Pseudomonas* sp. SHC52 (Fig. 3; see also Table S3). The amino acid sequence encoded by *nunE* and that encoded by the adjacent *nunD* ORF showed high similarity to the products of the thanamycin synthesis gene cluster from *Pseudomonas* sp. SHC52 (60% identity [Id] to ThaA and 76% Id to ThaB, respectively) as well as similarity to those of the syringomycin synthesis gene cluster (*syrE*) from *P. syringae* pv. *syringae* B728a, Cit7, and 642 (approximately [approx.] 30% to 40% Id) (Fig. 3; see also Table S3). In addition to *nunD* and *nunE*, the *nunB1* and *nunB2* gene products showed high similarity to the *thaC1* and *thaC2* gene products from *Pseudomonas* sp. SHC52 (73% and 87% Id, respectively) and to *syrB1* and *syrB2* gene products from *P. syringae* strains B728a, Cit7, and 642 (approx. 70% to 88% Id) (Fig. 3; see also Table S3). SyrB1/ThaC1 and SyrB2/ThaC2 are believed to be involved in selection and activation of Thr-9 and in chlorination of the nonribosomal peptides syringomycin and thanamycin, respectively (3, 12, 13). Furthermore, the *nunC* gene product showed high similarity to ThaD from *Pseudomonas* sp. SHC52 (69% Id) and to SyrC from *P. syringae* strains B728a, Cit7, and 642 (approx. 69% to 70% Id), which mediate the transfer of 4-Cl-L-Thr from the NRP-T1 domain to the NRP-T8,9 domain as described in the syringomycin synthesis assembly line (12). The peptide encoded by *nunB1*, *nunB2*, *nunC*, *nunD*, and *nunE* was denoted "nunamycin" (in Greenlandic, Nuna = Earth/land and Kalaallit Nunaat = Greenland).

Next to the nunamycin biosynthesis gene cluster, other ORFs

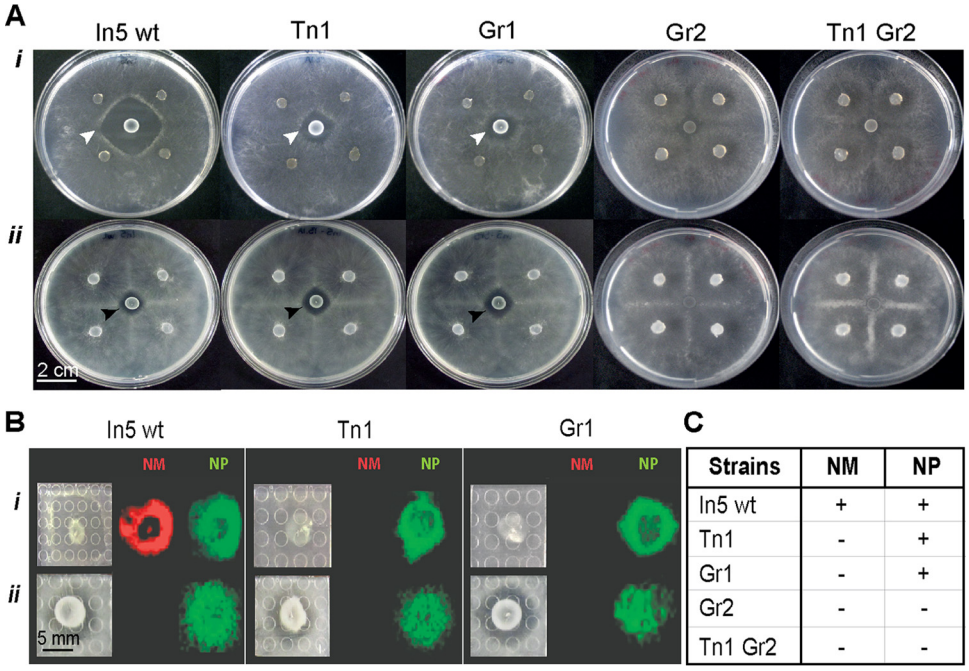

FIG 2 (A) Inhibition of *R. solani* Ag3 (*i*) or *P. aphanidermatum* (*ii*) mycelial growth by *P. fluorescens* In5 (wt) and the *P. fluorescens* In5-derived mutant strains, Tn1 (the *nunE* mutant), Gr1 (the *nunD* mutant), Gr2 (the *nupB* mutant), and Tn1 Gr2 (the *nunE nupB* double mutant). In all cases, the bacteria are seen in the central colony on the agar plate surrounded by four identical mycelium plugs. Inhibition of *R. solani* Ag3 is indicated by white arrowheads, whereas inhibition of *P. aphanidermatum* is indicated by black arrowheads. (B) MALDI-TOF imaging mass spectrometry images of nunamycin (NM; red) and nunapeptin (NP; green) produced by *P. fluorescens* In5 (wt) and the *P. fluorescens* In5-derived mutant strains, Tn1 and Gr1, cocultured with *R. solani* Ag3 (*i*) or *P. aphanidermatum* (*ii*). (C) Table summarizing production of nunamycin (NM) and nunapeptin (NP) by the *P. fluorescens* In5 wt and mutant strains Tn1, Gr1, Gr2, and Tn1Gr2 as evaluated by MALDI-TOF IMS and/or MS analysis. +, production of peptide; −, no production of peptide.

encoding putative NRPs were present. Three ORFs denoted *nupA*, *nupB*, and *nupC* displayed similarity to the syringopeptin biosynthesis gene cluster from *P. syringae* pv. *syringae* B728a (between 36% and 47% Id) (Fig. 3; see also Table S3 in the supplemental material), whereas a corresponding gene cluster was not identified in *Pseudomonas* sp. SHC52 due to a truncated DNA sequence from this isolate. The putative peptide encoded by the *nupA*, *nupB*, and *nupC* gene cluster was denoted nunapeptin. In addition to the two *nun* and *nup* gene clusters, the antifungal genomic island in *P. fluorescens* In5 also contained the genes *nupD*, *pseA* to *pseC* (*pseA-C*), and *pseE-F*, which in *P. syringae* have been associated with regulation and export of peptides (Fig. 3; see also Table S3) (14). The gene order of the In5 antifungal genomic island was identical to that of *P. syringae* pv. *syringae* B728a, but the *thaC1*, *thaC2*, and *thaD* genes in *Pseudomonas* sp. SHC52 were located downstream of the major NRP genes *thaA* and *thaB* (Fig. 3).

Gene replacement mutants Gr1 (mutated in *nunD*) and Gr2 (mutated in *nupB*) as well as a double mutant, Tn1Gr2, carrying both the mutation in Tn1 (mutated in *nunE*) and that in Gr2, were constructed in *P. fluorescens* In5 (Fig. 3) and analyzed for antifungal activities *in vitro* on agar plates. Mutant Gr1 displayed activity similar to that seen with mutant Tn1, i.e., significantly reduced inhibition of *R. solani* Ag3 mycelial growth compared to that of

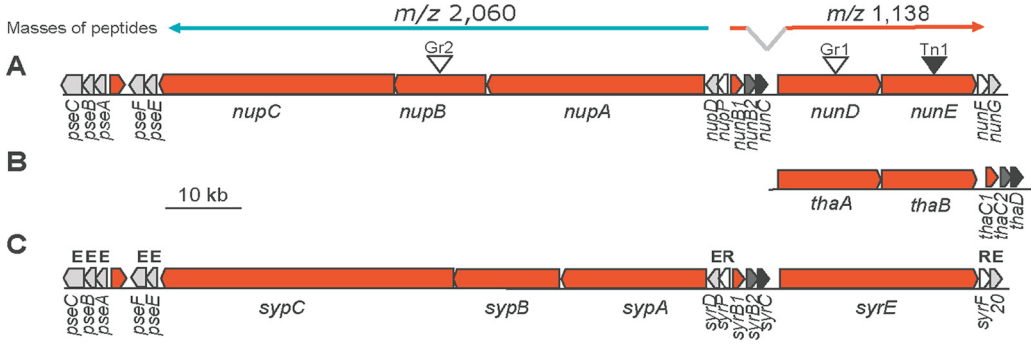

FIG 3 Map of the antifungal genome cluster of *P. fluorescens* In5 (A) and closest relatives *Pseudomonas* sp. SHC52 (GenBank accession no. HQ888764) (B) and *P. syringae* pv. *syringae* B728a (GenBank accession number NC_007005) (C). Open triangles show the gene replacement mutations corresponding to Gr1 and Gr2; the filled triangle shows the transposon mutation corresponding to Tn1. Grey arrow boxes with a boldface capital E denote genes involved in export; open arrow boxes with a boldface capital R denote genes involved in regulation.

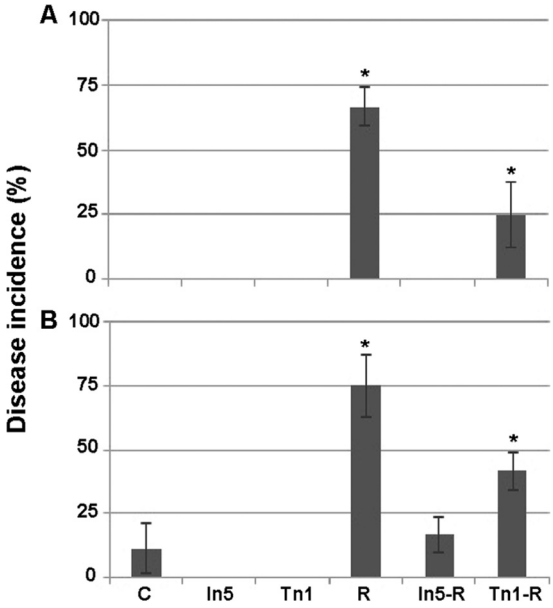

FIG 4 Soil microcosm experiment. The microcosm experiment was carried out with soil containing *R. solani* Ag3 (R) that was inoculated with *P. fluorescens* strain In5 wt and *R. solani* Ag3 (In5-R) or with mutant strain Tn1 and *R. solani* Ag3 (Tn1-R) and maintained at 15°C (A) or 20°C (B); the results were compared to those seen with untreated control soil (column C), soil inoculated with *P. fluorescens* In5 wt (In5) or mutant strain Tn1 (Tn1). Damping-off symptoms of infected seedlings caused by *R. solani* Ag3 were scored visually and expressed as percentages of disease incidence (means ± SEM, $n = 4$). Asterisks indicate statistically significant differences from the control treatment (column C) ($P < 0.05$, Tukey's HSD test).

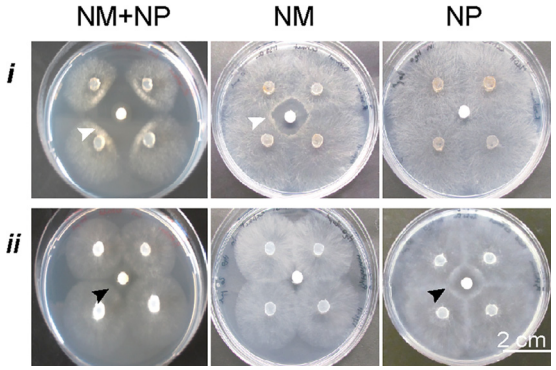

FIG 5 Inhibition of *R. solani* Ag3 (*i*) or *P. aphanidermatum* (*ii*) mycelial growth by 10 μg crude peptide extract derived from the *P. fluorescens* In5 wild type containing both the nunamycin and nunapeptin peptides (NM+NP); 10 μg of the purified nunamycin (NM) or nunapeptin (NP) peptides was spotted on sterile pieces of filter paper in the center of the agar plate surrounded by four identical mycelium plugs. Inhibition of *R. solani* Ag3 is indicated by white arrowheads, whereas inhibition of *P. aphanidermatum* is indicated by black arrowheads.

wild-type strain In5, whereas inhibition of *P. aphanidermatum* was slightly increased (Fig. 2A; see also Fig. S1 in the supplemental material). The biocontrol activity of the *nunE* mutant, Tn1, was further studied in soil microcosm experiments, and results revealed a substantially reduced ability to protect tomato seedlings against *R. solani* Ag3 compared to the wild-type In5 strain (Fig. 4). The *nupB* mutant, Gr2, had completely lost the ability to inhibit *P. aphanidermatum* mycelial growth, whereas the same low level of inhibition against *R. solani* Ag3 as that seen with the mutants Gr1 and Tn1 was observed (Fig. 2A; see also Fig. S1), indicating that, in contrast to the *nun* genes, *nupB* plays a role in biocontrol of *P. aphanidermatum*. Furthermore, the Tn1Gr2 double mutant showed virtually no *in vitro* inhibition activity against *R. solani* Ag3 or *P. aphanidermatum* (Fig. 2A; see also Fig. S1).

Identification of nonribosomal peptides produced by *P. fluorescens* In5 using MALDI-TOF imaging mass spectrometry. In order to bypass laborious and time-consuming conventional peptide purification methods, we used matrix-assisted laser desorption–ionization time of flight (MALDI-TOF) imaging mass spectrometry (IMS) to identify the antifungal peptides encoded by the antifungal genomic island in *P. fluorescens* In5. Ions of interest were selected by superimposing the false-colored ion distribution map from the IMS analysis onto an optical image of the bacterium-fungus interaction and searching for ions with a strong presence within the area of fungal inhibition (Fig. 2B and C). In cocultures of the *P. fluorescens* In5 wild type and *R. solani* Ag3, ions with a mass of *m*/*z* 1,138 and a family of *m*/*z* 2,023 to 2,075, with the highest intensity observed at *m*/*z* 2,060, were detected, whereas mutant strains Tn1 and Gr1 produced only the *m*/*z* 2,060 ion (Fig. 2B and C). These results showed that the *m*/*z* 1,138 ion corresponded to the nunamycin peptide and indicated that the *m*/*z* 2,060 ion corresponded to the nunapeptin peptide. MALDI-TOF mass spectrometry (MS) analysis of the *P. fluorescens* In5 wild type and the mutant strains further confirmed the production of both nunamycin and nunapeptin by the In5 wild-type strain, whereas the mutant strains, Tn1 and Gr1, produced only nunapeptin and, notably, the mutant strains, Gr2 and Tn1Gr2, showed no production of either nunamycin or nunapeptin (Fig. 2C; see also Fig. S2 in the supplemental material).

Surprisingly, we noticed in the MALDI-TOF IMS analysis that cocultures with *P. fluorescens* In5 and *P. aphanidermatum* showed the presence only of nunapeptin (i.e., *m*/*z* 2,060 ion) and not of nunamycin (i.e., *m*/*z* 1,138 ion) (Fig. 2B), indicating that *P. aphanidermatum* inhibited the synthesis of nunamycin in strain In5. Corroborating the results from coculture experiments, the crude peptide extract from *P. fluorescens* In5 containing both nunamycin and nunapeptin inhibited mycelial growth of both *R. solani* Ag3 and *P. aphanidermatum*, whereas the purified nunamycin peptide inhibited *R. solani* Ag3 but not *P. aphanidermatum*, and the purified nunapeptin in contrast showed inhibition of *P. aphanidermatum* but not of *R. solani* Ag3 (Fig. 5).

The expression of nunamycin and nunapeptin was analyzed over time using MALDI-TOF MS. The two ions *m*/*z* 1,138 and 2,060, corresponding to nunamycin and nunapeptin, respectively, first appeared 12 h after inoculation of *P. fluorescens* In5, with a maximum mass signal observed at 48 to 72 h (Fig. 6). In the two *nun* mutants, Tn1 and Gr1, the *m*/*z* 1,138 ion was absent (Fig. 6). After 7 days, the *m*/*z* 1,138 ion was no longer visible, whereas the *m*/*z* 2,060 ion was present but at a lower intensity (Fig. 6).

Molecular structures of nunamycin and nunapeptin reveal two cyclic lipopeptides. The molecular structures of nunamycin and nunapeptin are proposed on the basis of a combination of nuclear magnetic resonance (NMR)- and mass spectrometry (MS)-based methods (Fig. 7). For nunamycin, initial analysis of the parent peak at *m*/*z* 1,138.54 by high-resolution mass spectrometry indicated the presence of a single chlorine atom within

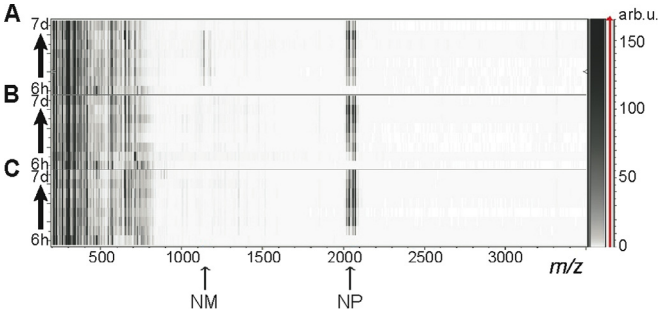

FIG 6 Time course experiments with the *P. fluorescens* In5 wild type (A) and the mutant strains, *P. fluorescens* Tn1 (B) and *P. fluorescens* Gr1 (C), cultured on solid 1/5 PDA. Production of nunamycin (NM) (i.e., *m/z* 1,138) and members of the nunapeptin family (NP) (i.e., *m/z* 2,060) by the bacterial strains was measured using MALDI-TOF dried-droplet mass spectrometry at 6 h, 12 h, 24 h, 36 h, 48 h, 72 h, 96 h, and 7 days (d) of incubation as indicated by each line on the *y* axis. Mass spectra are displayed as stacked heat maps. Each numbered row is a single mass spectrum with peak intensities represented as a color scale, where low-intensity signals are closer to white and higher-intensity signals are closer to black as shown in the panel to the right of the spectrum. arb.u., arbitrary units.

the structure due to a 24% increase in the M +2 peak due to the ^{37}Cl isotope of chlorine. Analysis of the gene cluster also showed the presence of a chlorinase enzyme adjacent to an adenylation domain capable of loading a 4-Cl threonine residue (see Fig. S3 in the supplemental material). Analysis of the nunamycin gene cluster and comparisons to the syringomycin and thanamycin gene clusters indicated a missing A domain in the modular organization of the nunamycin NRP (i.e., in module 5 as shown in Fig. S3); at the same time, further annotation of NMR, tandem MS (MS/MS), and MS/MS/MS data revealed that nunamycin is a cyclic lipopeptide, consistent with the presence of the 9 amino acid residues Ser-Dab-Gly-Hse-Dab-Thr-Thr-(3-OH)Asp-(4-Cl-Thr) (see the Fig. 7 legend for definitions of abbreviations) attached to a 3-hydroxy fatty acid tail (Fig. 7; see also Fig. S3).

Analysis of the nunapeptin gene cluster combined with MS/MS analysis revealed the presence of a 22-amino-acid cyclic lipopeptide, i.e., Dhb-Pro-Ala-Ala-Ala-Val-Ala-Dhb-Ser-Val-Ile-Dha-Ala-Val-Ala-Val-Dhb-Thr-Ala-Dab-Ser-Ile, with strong similarity to corpeptin and syringopeptin (Fig. 7; see also Fig. S4 in the supplemental material). By high-resolution mass spectrometry, the primary ion at *m/z* 2,045.20 gave a clear sequence tag for 16 amino acid residues with the sequence Pro-Ala-Ala-Ala-Val-Ala-Dhb-Ser-Val-Ile-Dha-Ala-Val-Ala-Val-Thr. In addition, two larger fragments at *m/z* 254.175 and *m/z* 473.272 appeared in the mass spectrum. The molecular formula of the *m/z* 254.175 fragment correlated with a Dhb residue attached to 3-OH dodecanoic acid (Fig. 7; see also Fig. S4), which is similar to the structure of syringopeptin and corpeptin (15). The molecular formula for the *m/z* 473.272 fragment was consistent with a Thr-Ala-Dab-Ser-Ile cyclic peptide moiety (Fig. 7; see also Fig. S4), which is identical to the cyclic tail of corpeptin (15). The results of two-dimensional (2D) homo- and heteronuclear NMR experiments supported the mass spectral interpretation (see Table S4). In addition to the primary nunapeptin, three analogs were observed in the mass spectrum of In5 (*m/z* 2,023.22, *m/z* 2,037.24, and *m/z* 2,075.22) (see Fig. S2). Tandem MS analysis of these analogs showed identical mass losses for the lipid tail (*m/z* 254.175) as well as for the terminal cyclic peptide (*m/z* 473.272).

DISCUSSION

In certain subarctic fields in Greenland, it is possible to cultivate potatoes with limited crop rotation and no use of pesticides, even though plant-pathogenic fungi are present in the soils. Using soil microcosms, we showed that a potato soil from Inneruulalik in southern Greenland was able to suppress the growth of the plant-pathogenic fungus *Rhizoctonia solani* Ag3. Such suppressive soils exist worldwide (2), but this report is the first to describe a disease-suppressive soil from a subarctic region. Antifungal microorganisms from suppressive soils have been shown to comprise several bacterial genera (2, 8–11), and an analysis of the Inneruulalik soil by 16S rRNA gene pyrosequencing identified the presence of organisms belonging to several of these genera, i.e., *Pseudomonas*, *Bacillus*, *Paenibacillus*, *Streptomyces*, and *Burkholderia*. However, the frequency of organisms of these genera constituted in total less

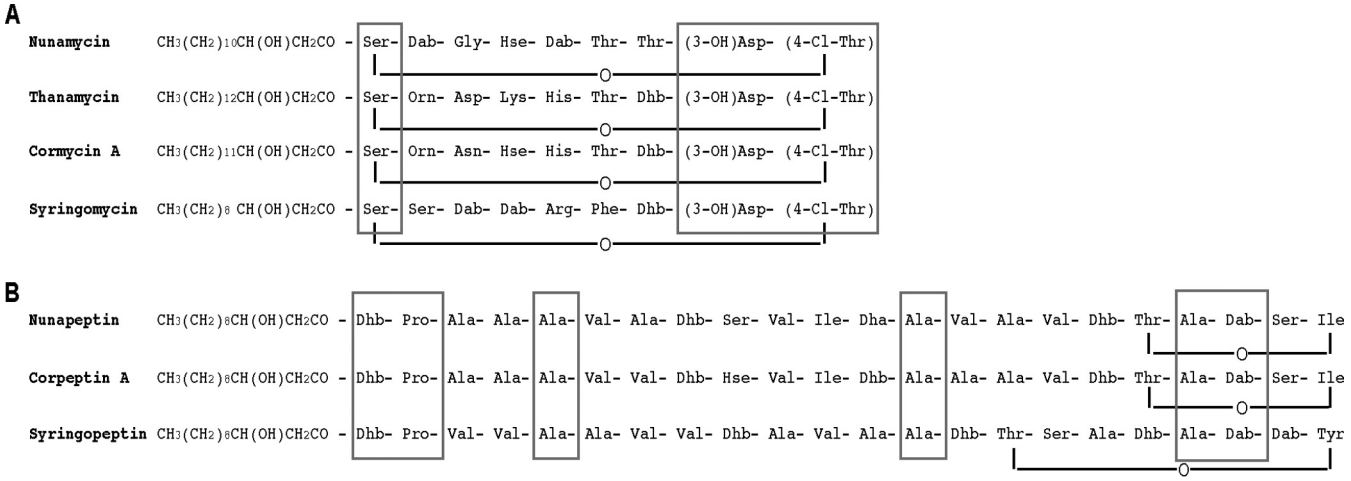

FIG 7 The proposed structures of nunamycin from *P. fluorescens* In5 and the analogous peptides thanamycin, cormycin A, and syringomycin (A) and of nunapeptin from *P. fluorescens* In5 and the analogous peptides corpeptin A and syringopeptin (B). The abbreviations are as follows: (3-OH)Asp, 3-hydroxyaspartic acid; (4-Cl)Thr, 4-chlorothreonine; Dab, 2,4-diaminobutyric acid; Dhb, dehydrobutyrine; Dha, dehydroalanine; Orn, ornithine; Hse, homoserine. Consensus amino acids are denoted in gray-lined boxes.

than 1% of all phylotypes, which led us to the assumption that the bacteria present in the disease-suppressive Inneruulalik soil must be potent inhibitors of fungal growth. An effective biocontrol bacterium, *P. fluorescens* In5, was previously isolated from the Inneruulalik soil and was found to encode genes for the synthesis of antifungal compounds, including hydrogen cyanide and a hitherto-uncharacterized nonribosomal peptide (6, 7).

Nonribosomal peptides isolated from several pseudomonads using conventional methods such as extraction of active compounds in organic solvents followed by high-pressure liquid chromatography (HPLC) fractionation and structure resolution by NMR and MS have been described previously (16–18). In this study, we demonstrated that molecular genetics combined with genomics and MALDI-TOF IMS may facilitate the process of identification and purification of NRPs and in addition assist in verifying the presence of the desired compounds within the different extraction and purification steps. Furthermore, this approach facilitated expression studies of the individual NRPs in live bacterial-fungal cocultures both spatially and temporally. MALDI-TOF IMS analysis of *P. fluorescens* In5 revealed the presence of two antifungal NRPs in the inhibition zone of *R. solani* AG3 and *P. aphanidermatum*, respectively. These NRPs, denoted nunamycin and nunapeptin, showed structural resemblance to syringomycin and syringopeptin from *P. syringae* and to cormycin A and corpeptin A from *P. corrugata* (15) as well as to thanamycin from *Pseudomonas* sp. SH-C52 (19). Nunamycin was found to be a chlorinated cyclic lipopeptide composed of 9 amino acid residues, Ser-Dab-Gly-Hse-Dab-Thr-Thr-(3-OH)Asp-(4-Cl-Thr), with a molecular mass of 1,137.54 Da, while nunapeptin was produced as a family of cyclic lipopeptides of 22 amino acid residues, Dhb-Pro-Ala-Ala-Ala-Val-Ala-Dhb-Ser-Val-Ile-Dha-Ala-Val-Ala-Val-Dhb-Thr-Ala-Dab-Ser-Ile, with molecular masses ranging from 2,023 to 2,075 Da. The structures of nunamycin and nunapeptin contained some uncommon amino acids, such as (3-OH)Asp (3-hydroxyaspartic acid), (4-Cl)Thr (4-chlorothreonine), Dab (2,4-diaminobutyric acid), Dhb (dehydrobutyrine), and Dha (dehydroalanine). However, these amino acids are present in a range of nonribosomal peptides, including antimicrobial peptides of the syringomycin, tolaasin, and syringopeptin families (15).

While the biosynthesis of nunapeptin is catalyzed by three NRPs (NupA, NupB, and NupC) in a collinear manner, the biosynthesis of nunamycin, catalyzed by the three NRPs, NunB1/NunB2, NunD, and NunE, does not respect the collinearity rule. For example, a split-module phenomenon was found in the ninth module in the nunamycin NRP, NunE; the C and T domains were present, but an A domain was not, which instead was present in NunB1, as also described for the syringomycin synthase (15). Furthermore, an additional A domain was lacking in module 5 of the nunamycin NRP NunD. However, chemical analysis showed that Dab was present as the fifth amino acid in the nunamycin peptide chain; thus, we speculate that the A domain in module 2 could function twice. Such module shuffling has been documented before in NRP-catalyzed peptide synthesis (20).

Transposon and gene replacement mutants, i.e., Tn1, Gr1, Gr2, and Tn1Gr2, constructed in *P. fluorescens* In5 confirmed that nunamycin and nunapeptin are key components for the biocontrol ability observed by this strain. However, the two peptides showed distinct inhibition activities. Nunamycin was found to play a role primarily in *R. solani* AG3 mycelial growth inhibition, whereas nunapeptin was essential for *P. aphanidermatum* inhibition. However, when a nunapeptin NRP knockout mutant (Gr2, mutated in *nupB*) was analyzed in coculture, this mutant was defective in growth inhibition of both *P. aphanidermatum* and *R. solani* Ag3, although the nunamycin biosynthesis was intact. A closer examination of the *nup* operon showed the presence of six genes, *nupD*, *pseA-C*, and *pseE-F*, possibly involved in the efflux of NRPs (14, 21). Thus, it is likely that the knockout of the *nupB* gene in *P. fluorescens* In5 negatively influences not only the synthesis of nunapeptin but also the efflux system located downstream of the *nup* genes. If expression of the *pse* genes is affected, this could inhibit efflux of both the nunapeptin and nunamycin and consequently also affect the inhibition activity against both *P. aphanidermatum* and *R. solani* Ag3. This hypothesis was supported by MALDI-TOF MS analysis, which showed no production of nunapeptin or nunamycin by this mutant strain.

MALDI-TOF IMS enabled us to study the expression of nunamycin and nunapeptin simultaneously and in relation to interactions between *P. fluorescens* In5 and *R. solani* Ag3 or *P. aphanidermatum*. Nunamycin and nunapeptin were both expressed in cocultures of *P. fluorescens* In5 with *R. solani* Ag3. However, only nunapeptin was present in cocultures with *P. aphanidermatum*, suggesting that the synthesis of nunamycin in *P. fluorescens* In5 was inhibited by *P. aphanidermatum*. Regulation of lipopeptides and other secondary metabolites in pseudomonads by other organisms has been reported in several cases. For example, the production of secondary metabolites in *P. aeruginosa* was found to be affected by a halogenated furanone compound produced by the Australian macroalga *Delisea pulchra* (22), and sugar beet extracts were shown to affect lipopeptide synthesis in *Pseudomonas* sp. DSS73 (23). The exact mechanism by which *P. aphanidermatum* inhibited the biosynthesis of nunamycin in *P. fluorescens* In5 in this study, however, still needs to be elucidated.

MALDI-TOF MS analysis similarly permitted a study of the expression of nunamycin and nunapeptin by *P. fluorescens* In5 wild-type and mutant strains and allowed a time course analysis of nunamycin and nunapeptin synthesis by *P. fluorescens* In5. Nunamycin and nunapeptin were first detected 12 h after inoculation, with signals for the peptides reaching a maximum after 48 to 72 h of incubation and subsequently decreasing after 7 days of incubation. This expression profile is different from other lipopeptide synthesis profiles. For example, in *P. fluorescens* strain SS101, massetolide A biosynthesis initiates between 12 h and 16 h of incubation and peaks after 24 h of incubation (24). In *Bacillus amyloliquefaciens*, synthesis of surfactin and fengycin displayed maximal production after 10 to 40 h and decreased after 60 h, whereas bacillomycin D showed maximal intensity after 40 and 60 h (25). The transient production of nunamycin, however, has previously been observed with the analogous molecule thanamycin from *Pseudomonas* sp. SH-C52 (19).

The results presented in this report demonstrate the powerful approach of combining *in vitro* inhibition experiments with molecular genetics, genomics, and MALDI-TOF IMS analyses. Using this combination of tools, we were able to unravel the key biocontrol factors of a Greenlandic bacterium, *P. fluorescens* In5, isolated from a disease-suppressive potato soil in subarctic Greenland, to elucidate the structure and function of two antifungal lipopeptides, and to document that the effective biocontrol ability of *P. fluorescens* In5 requires the synthesis of both peptides.

TABLE 1 Bacteria, fungi, and plasmids used in this study

Plasmid or bacterial or fungal strain	Relevant genotype and (or) characteristic(s)[a]	Reference
Plasmids		
ppiKmLacZ	Km^r-*lacZ* cassette; pTnMod-based; mobilizable	26
pRK2013	Self-transmissible helper plasmid; Km^r	27
pEX100T	*oriT*, *bla*, *sacB*	28
Bacteria		
Escherichia coli DH5α	*endA1 hsdR17 supE44 thi-1 recA1 U169 deoR*	34
Pseudomonas fluorescens In5	WT	6
Pseudomonas fluorescens In5-Tn1	Δ*nunE*	6
Pseudomonas fluorescens In5-Gr1	Δ*nunD*	This study
Pseudomonas fluorescens In5-Gr2	Δ*nupB*	This study
Pseudomonas fluorescens In5-Tn1Gr2	Δ*nunE* Δ*nupB*	This study
Fungus or oomycete		
Rhizoctonia solani Ag3	Basidiomycete	6
Pythium aphanidermatum	Oomycete	6

[a] Km, kanamycin; WT, wild type.

MATERIALS AND METHODS

Strains and culture conditions. Bacterial strains (Table 1) were routinely grown in liquid or on solid (1.5% agar) Luria-Bertani (LB) medium at 28°C (*Pseudomonas* strains) or at 37°C (*Escherichia coli* [for transposon mutagenesis]). When required, the medium was supplemented with the following antibiotic(s): kanamycin (50 $\mu g \cdot ml^{-1}$), ampicillin (50 $\mu g \cdot ml^{-1}$), or gentamicin (10 $\mu g \cdot ml^{-1}$). The basidiomycete *R. solani* Ag3 and the oomycete *P. aphanidermatum* (Table 1) were used as target pathogens in *in vitro* inhibition assays and soil microcosm experiments. The fungus or oomycete was maintained on standard potato dextrose agar (PDA; BD/Difco, USA) medium at 20°C.

Soil sampling, DNA isolation, and pyrosequencing analysis of the Inneruulalik potato soil. For details on soil sampling, DNA isolation, and pyrosequencing analysis of the Inneruulalik potato soil, see Materials and Methods in the supplemental material.

Soil microcosm assays. The Inneruulalik soil was sieved (0.5-cm-pore-size mesh) to remove plant debris and small stones. Tomato seeds (cv. Marmande Super) were presprouted for 4 days at 20°C in petri dishes on wetted filter paper.

For determination of soil suppressiveness, four presprouted tomato seedlings were placed randomly in petri dishes filled with 40 g of soil with an initial moisture content of 14.8% (vol/wt). The various soil treatments were suppressive soil (S), suppressive soil heat-treated at 80°C in an oven for 1 h (C), and heat-treated soil mixed with 10% (wt/wt) suppressive soil (CS). *R. solani* Ag3 was introduced into the soil by transferring one quarter of a mycelium agar plug (6-mm diameter) of a 1-week-old PDA plate to each corner of a petri dish. Plates were incubated in a growth chamber at 15°C using a 16-h:8-h light:dark cycle and watered after 1 week of incubation with 5 ml of standard Hoagland solution (macronutrients only). Four replicates (i.e., plates) were made for each soil treatment, and the experiment was repeated twice. After 12 days of incubation, the percentage of infected tomato seedlings showing damping-off symptoms was scored.

In order to determine the *R. solani* Ag3-suppressive activity by the *P. fluorescens* In5 wild type and the *P. fluorescens* Tn1 mutant strain, soil was initially heat-treated at 80°C in an oven for 1 h. Four presprouted tomato seedlings were placed randomly in petri dishes filled with 40 g of the heat-treated soil with or without addition (2 ml/100 g) of overnight (O/N) bacterial cultures washed twice with LB and adjusted to an optical density at 600 nm (OD_{600}) of 2. *R. solani* Ag3 was introduced into the soil as described above. The various soil treatments were control soil, tomato seedlings only (C), soil inoculated with the *P. fluorescens* In5 wild type (In5), soil inoculated with mutant strain *P. fluorescens* Tn1 (Tn1), soil infected with *R. solani* Ag3 (R), soil inoculated with the *P. fluorescens* In5 wild type and infected with *R. solani* Ag3 (In5-R), and soil inoculated with mutant strain *P. fluorescens* Tn1 and infected with *R. solani* Ag3 (Tn1-R). Plates were incubated in a growth chamber at 15°C or 20°C with a 16-h:8-h light:dark cycle. Plates were watered as described above. Four replicates (i.e., plates) were made for each soil treatment, and the experiment was repeated twice. After 10 and 6 days of incubation at 15°C and 20°C, respectively, the percentage of infected tomato seedlings showing damping-off symptoms was scored.

Screening of the transposon mutant library. Transposon mutagenesis of *P. fluorescens* In5 was performed using a mobilizable plasposon, pTn*Mod*OKm (26), as previously described (27). Strain In5 transconjugants with transposons integrated into the chromosome were selected on LB agar plates supplemented with kanamycin and ampicillin. Approximately 1,500 mutants were screened for lack of antifungal activity. Mutants were grown O/N in F96 Microwell plate (Nunc) (in 150 μl LB with ampicillin [50 $\mu g \cdot ml^{-1}$ per well] and kanamycin [50 $\mu g \cdot ml^{-1}$ per well]). Overnight cultures (1.5 μl) were transferred by a multichannel pipette to OmniTrays (Nunc) containing PDA at a strength of 1/5 (1/5 PDA) previously inoculated with a suspension of blended fungal hyphae of *R. solani* Ag3 or *P. aphanidermatum*. Transposon rescue of selected mutants using XhoI or SacII was performed as previously described (6).

Homologous recombination. Gene knockout by homologous recombination in the *m/z* 1,138 and *m/z* 2,060 NRP gene clusters was carried out using a gene replacement vector, pEX100T (28). Approximately 2,000 to 2,300 bp of the *m/z* 1,138 and *m/z* 2,060 NRP gene clusters containing one or two SalI sites were amplified with primers NRPS13a (5′-CGCATAAC CGCACACTG′-3) and NRPS13b (5′-CTGGAACAAGTCGGTCGC′-3) and primers 2 F (5′-TGTCGAGGCTTGCGCCAAC′-3) and 2 R (5′-CG CGGAAGCGGTGATCCT′-3), respectively. The *m/z* 1,138 and *m/z* 2,060 NRP gene fragments were amplified using Phusion blunt-end polymerase (annealing temperature, 63°C), according to the manufacturer's instructions. The blunt-end-amplified fragments were ligated into SmaI-digested pEX100T. The pEX100T vectors with insertions were digested with SalI, and a SalI-digested gentamicin resistance (Gm^r) gene and a promoter from plasmid Tn7gfp2 (29) were inserted into the NRP gene clusters. The pEX100T vectors with NRP fragments disrupted by the Gm^r gene were transformed into electrocompetent *P. fluorescens* In5 cells together with the pUX-BF13 helper plasmid as previously described (30). Strain In5 transformants with a site-directed knockout in one of the two NRP gene clusters were selected on LB agar plates supplemented with ampicillin and gentamicin.

Fungus/oomycete inhibition assays on agar plates. Antifungal activity of the different strains and the purified nunamycin and nunapeptin was tested on 1/5 PDA against *R. solani* Ag3 or *P. aphanidermatum*. Ten

microliters of O/N bacterial cultures or 10 μg of the crude peptide extract or purified nunamycin and nunapeptin peptides on sterile filter papers was inoculated in the center of the agar plates. Sterile MilliQ purified H_2O on filter paper was used as a control for the peptide extract and purified peptides. Four fungus/oomycete mycelium plugs were placed 2 cm from the center of the plate around the colony or filter paper. Plates were made in triplicate and incubated at 15°C (*P. aphanidermatum*) or 20°C (*R. solani* Ag3). Following 48 to 240 h of coculturing, depending on the fungus/oomycete strain and incubation temperature used, all plates were visually inspected and the inhibitory effect of the bacterial strains was evaluated as percent inhibition of radial growth (PIRG) as previously described (31).

MALDI-TOF imaging mass spectrometry analysis. *P. fluorescens* In5 or mutant strain Tn1 or Gr1 was cocultured with *R. solani* Ag3 or *P. aphanidermatum* on thin 1/5 PDA plates (i.e., 10 ml of media in a standard petri dish, resulting in a thickness of medium of about 1.5 mm). Once the desired time point for growth was reached, areas of agar media containing the microbial colonies were excised from the petri dish and transferred to the MALDI stainless steel target plate. The subsequent matrix application was performed using a 53-μm-pore-size test sieve; dry matrix was deposited evenly across the sample surface until the desired matrix thickness was achieved. The sample was dried O/N followed by MALDI-TOF IMS analysis using a Bruker Microflex mass spectrometer. Data were collected from 50 to 3,000 *m/z* at 80-Hz laser frequency at a spatial resolution of 400 μm using a random-walk shot pattern. Data were analyzed using the Compass 1.2 software suite (FlexImaging 2.0, FlexControl 3.0, and FlexAnalysis 3.0; Bruker Daltonics) as previously described (32). The resulting mass spectrum was binned at 0.5-m/*z* increments and manually inspected for masses of interest. Masses were visualized using false coloring on an optical image of the original sample plate.

Peptide extraction. Plates with 1/5 PDA medium were inoculated with *P. fluorescens* In5. After incubation for 48 h at room temperature, the agar was sliced into small pieces and extracted with acidified deionized water (pH 2) for 1 h at 28°C and 225 rpm in a 2.8-liter Erlenmeyer flask followed by addition of n-butanol and incubation for 18 h at 28°C. The n-butanol extract was separated from agar by cheesecloth filtration and subsequently from cell debris by centrifugation (6,440 × *g*, 10 min). n-Butanol was removed with a rotovaporator (Buechi R-200). The crude peptide extract was resuspended in 1 ml methanol and analyzed by MALDI-TOF mass spectrometry (MS). The resuspended extract was centrifuged for 2 min at 16,000 × *g*, and the supernatant was placed on a methanol-equilibrated Sephadex LH20 column (30 cm length). The peptide extract was separated with a methanol mobile phase at a flow rate of 0.4 ml/min. Fractions of 7.5 ml were collected, lyophilized, and resuspended in 200 μl methanol. Gel filtration fractions were analyzed by MALDI-TOF MS for peptide content. Fractions of the peptide-containing gel filtration were combined and concentrated by lyophilization. The peptides were further purified by reversed-phase high-pressure liquid chromatography (HPLC) using an Agilent 1260 system equipped with a Phenomenex Kinetex C_{18} column (4.6 mm by 15 cm). The peptides were eluted from the column using a gradient of 10% acetonitrile containing 0.1% formic acid:90% water containing 0.1% formic acid to 90% acetonitrile containing 0.1% formic acid:10% water containing 0.1% formic acid over 45 min at a flow rate of 1.0 ml/min. Peaks for nunamycin and nunapeptin were collected manually (24.6 min for nunamycin and multiple peaks between 35 and 40 min for the nunapeptin family of compounds), after which they were lyophilized and stored at −80°C.

NMR and tandem MS analysis. About 1 mg of nunapeptin at *m/z* 2,023 to 2,075 and about 100 μg of nunamycin at *m/z* 1,138 were dissolved in 40 μl of deuterated methanol (CD_3OD) for NMR data acquisition. NMR spectra were recorded on a Bruker Avance iii 600-Mhz spectrometer with a 1.7-mm-diameter Microbiology CryoProbe at 298 K, with standard pulse sequences provided by Bruker. Structures were confirmed by analysis of 1D proton, 2D Cosy double-quantum filter (Dqf-Cosy), 2D 1H-13C heteronuclear single-quantum coherence (HSQC), and 2D 1H-13C heteronuclear multiple-bond correlation (HMBC) spectra. 2D 1H-13C HMBC spectra were recorded with delays corresponding to a 2j or 3j H-C coupling constant of 8 Hz and a 1j H-C coupling constant of 145 Hz. 2D 1H-13C multiplicity-edited HSQC spectra were recorded, with delays corresponding to a 1j H-C coupling constant of 140 Hz. Spectra were referenced to the methanol methyl resonance at 3.31 ppm.

Tandem mass spectrometry experiments were performed on a Thermo LTQ fault-tolerant (FT) mass spectrometer (Thermo Electron Corp., Bremen, Germany) equipped with a Diversa Nanomate electrospray source. Aliquots from solutions of purified nunapeptin and nunamycin compounds were diluted in acetonitrile:0.1% formic acid (70:30 [vol/vol]). Electrospray parameters included a spray voltage of 1.40 kV, heated inlet temperature of 200°C, nebulizing gas pressure of 40 lb/in^2 N_2, collision-induced dissociation energy of 25 V, and collision time of 500 ms. The instrument was operated in FT mode (peak resolution, 50 k) for detection of parent (MS) and daughter (MS/MS) ion peaks.

MALDI-TOF mass spectrometry. MALDI-TOF MS was used to detect target peptides in the crude peptide extract and fractions from gel filtration and HPLC as well as peptide production over time in the time course experiment. The sample was mixed 1:1 with a saturated solution of Universal MALDI matrix–70% acetonitrile containing 0.1% trifluoroacetic acid (TFA) and spotted on a Bruker MSP 96 anchor plate. The target plate containing the samples was dried and inserted into a Microflex Bruker Daltonics mass spectrometer. External calibration was done as described for MALDI-TOF IMS. Mass spectra were obtained with the FlexControl method as used for MALDI-TOF IMS and a single-spot acquisition of 200 shots. Single-spot MALDI-TOF MS data were analyzed by FlexAnalysis software.

Time course experiment of peptide production. Cultures of the *P. fluorescens* In5 wild type and the mutant strains, *P. fluorescens* Tn1 and Gr1, were inoculated on solid 1/5 PDA at 20°C and sampled at specific time points. Samples for dry-droplet analysis of peptide production (*m/z* 1,138 and 2,060) by MALDI-MS were taken after 6, 12, 24, 36, 48, 72, and 96 h and after 7 days. A scrape of bacterial colonies was dissolved in 100 μl of sterile deionized water. The bacterial suspension was mixed 1:1 with a saturated solution of Universal MALDI matrix in 70% acetonitrile containing 0.1% TFA and spotted on a Bruker MSP 96 anchor plate. MALDI MS analysis was carried out as described above.

Statistical analysis. Tukey's honestly significant difference (HSD) test was used in conjunction with analysis of variance (ANOVA) in order to evaluate the data from the *in vitro* inhibition and microcosm experiments to identify means with significant differences. The tests were carried out with R version 2.10.0 (33).

SUPPLEMENTAL MATERIAL

Supplemental material for this article may be found at http://mbio.asm.org/lookup/suppl/doi:10.1128/mBio.00079-15/-/DCSupplemental.

Text S1, DOC file, 0.01 MB.
Figure S1, PDF file, 1 MB.
Figure S2, PDF file, 0.2 MB.
Figure S3, PDF file, 0.2 MB.
Figure S4, PDF file, 0.3 MB.
Table S1, PDF file, 0.2 MB.
Table S2, PDF file, 0.1 MB.
Table S3, PDF file, 0.1 MB.
Table S4, PDF file, 0.1 MB.

ACKNOWLEDGMENTS

Referring to the Convention on Biological Diversity, we thank the government of Greenland and the Greenlandic farmers for permission to sample soil and bacteria in southern Greenland.

We thank Laura Sanchez for consultations on the NMR analysis.

This work was funded in part by the Commission for Scientific Research in Greenland and the Augustinus Foundation and NIH GM097509, NIHAI095125, and S10RR029121.

REFERENCES

1. **Raaijmakers JM, Paulitz TC, Steinberg C, Alabouvette C, Moënne-Loccoz Y**. 2009. The rhizosphere: a playground and battlefield for soilborne pathogens and beneficial microorganisms. Plant Soil **321:**341–361. http://dx.doi.org/10.1007/s11104-008-9568-6.
2. **Weller DM, Raaijmakers JM, Gardener BB, Thomashow LS**. 2002. Microbial populations responsible for specific soil suppressiveness to plant pathogens. Annu Rev Phytopathol **40:**309–348. http://dx.doi.org/10.1146/annurev.phyto.40.030402.110010.
3. **Mendes R, Kruijt M, de Bruijn I, Dekkers E, Mendes R, Kruijt M, de Bruijn I, Dekkers E, van der Voort M, Schneider JH, Piceno YM, DeSantis TZ, Andersen GL, Bakker PA, Raaijmakers JM**. 2011. Deciphering the rhizosphere microbiome for disease-suppressive bacteria. Science **332:**1097–1100. http://dx.doi.org/10.1126/science.1203980.
4. **Yuen GY, Schroth MN**. 1986. Inhibition of *Fusarium oxysporum* f. sp. *dianthi* by iron competition with an *Alcaligenes* sp. Phytopathology **76:**171–176. http://dx.doi.org/10.1094/Phyto-76-171.
5. **Haas D, Défago G**. 2005. Biological control of soil-borne pathogens by fluorescent pseudomonads. Nat Rev Microbiol **3:**307–319. http://dx.doi.org/10.1038/nrmicro1129.
6. **Michelsen CF, Stougaard P**. 2011. A novel antifungal *Pseudomonas fluorescens* isolated from potato soils in Greenland. Curr Microbiol **62:**1185–1192. http://dx.doi.org/10.1007/s00284-010-9846-4.
7. **Michelsen CF, Stougaard P**. 2012. Hydrogen cyanide synthesis and antifungal activity of the biocontrol strain *Pseudomonas fluorescens* In5 from Greenland is highly dependent on growth medium. Can J Microbiol **58:**381–390. http://dx.doi.org/10.1139/w2012-004.
8. **Lemanceau P, Alabouvette C**. 1991. Biological control of *Fusarium* diseases by fluorescent *Pseudomonas* and nonpathogenic *Fusarium*. Crop Protect **10:**279–286. http://dx.doi.org/10.1016/0261-2194(91)90006-D.
9. **Ongena M, Jacques P**. 2008. *Bacillus* lipopeptides: versatile weapons for plant disease biocontrol. Trends Microbiol **16:**115–125. http://dx.doi.org/10.1016/j.tim.2007.12.009.
10. **Son SH, Khan Z, Kim SG, Kim YH**. 2009. Plant growth-promoting rhizobacteria, *Paenibacillus polymyxa* and *Paenibacillus lentimorbus* suppress disease complex caused by root-knot nematode and fusarium wilt fungus. J Appl Microbiol **107:**524–532. http://dx.doi.org/10.1111/j.1365-2672.2009.04238.x.
11. **Raaijmakers JM, Mazzola M**. 2012. Diversity and natural functions of antibiotics produced by beneficial and plant pathogenic bacteria. Annu Rev Phytopathol **50:**403–424. http://dx.doi.org/10.1146/annurev-phyto-081211-172908.
12. **Guenzi E, Galli G, Grgurina I, Gross DC, Grandi G**. 1998. Characterization of the syringomycin synthetase gene cluster—a link between prokaryotic and eukaryotic peptide synthetases. J Biol Chem **273:**32857–32863. http://dx.doi.org/10.1074/jbc.273.49.32857.
13. **Vaillancourt FH, Yin J, Walsh CT**. 2005. SyrB2 in syringomycin E biosynthesis is a nonheme FeII alpha-ketoglutarate- and O2-dependent halogenase. Proc Natl Acad Sci U S A **102:**10111–10116. http://dx.doi.org/10.1073/pnas.0504412102.
14. **Cho H, Kang H**. 2012. The PseEF efflux system is a virulence factor of *Pseudomonas syringae* pv. *syringae*. J Microbiol **50:**79–90. http://dx.doi.org/10.1007/s12275-012-1353-9.
15. **Gross H, Loper JE**. 2009. Genomics of secondary metabolite production by *Pseudomonas* spp. Nat Prod Rep **26:**1408–1446. http://dx.doi.org/10.1039/b817075b.
16. **Gerard J, Lloyd R, Barsby T, Haden P, Kelly MT, Andersen RJ**. 1997. Massetolides A H, antimycobacterial cyclic depsipeptides produced by two pseudomonads isolated from marine habitats. J Nat Prod **60:**223–229. http://dx.doi.org/10.1021/np9606456.
17. **Saini HS, Barragán-Huerta BE, Lebrón-Paler A, Pemberton JE, Vázquez RR, Burns AM, Marron MT, Seliga CJ, Gunatilaka AA, Maier RM**. 2008. Efficient purification of the biosurfactant viscosin from *Pseudomonas libanensis* strain M9–3 and its physicochemical and biological properties. J Nat Prod **71:**1011–1015. http://dx.doi.org/10.1021/np800069u.
18. **De Bruijn I, de Kock MJ, de Waard P, van Beek TA, Raaijmakers JM**. 2008. Massetolide A biosynthesis in *Pseudomonas fluorescens*. J Bacteriol **190:**2777–2789. http://dx.doi.org/10.1128/JB.01563-07.
19. **Watrous J, Roach P, Alexandrov T, Heath BS, Yang JY, Kersten RD, van der Voort M, Pogliano K, Gross H, Raaijmakers JM, Moore BS, Laskin J, Bandeira N, Dorrestein PC**. 2012. Mass spectral molecular networking of living microbial colonies. Proc Natl Acad Sci U S A **109:**E1743–E1752. http://dx.doi.org/10.1073/pnas.1203689109.
20. **Barkei JJ, Kevany BM, Felnagle EA, Thomas MG**. 2009. Investigations into viomycin biosynthesis by using heterologous production in *Streptomyces lividans*. Chembiochem **10:**366–376. http://dx.doi.org/10.1002/cbic.200800646.
21. **Quigley NB, Mo YY, Gross DC**. 1993. SyrD is required for syringomycin production by *Pseudomonas syringae* pathovar *syringae* and is related to a family of ATP-binding secretion proteins. Mol Microbiol **9:**787–801. http://dx.doi.org/10.1111/j.1365-2958.1993.tb01738.x.
22. **Hentzer M, Riedel K, Rasmussen TB, Heydorn A, Andersen JB, Parsek MR, Rice SA, Eberl L, Molin S, Høiby N, Kjelleberg S, Givskov M**. 2002. Inhibition of quorum sensing in *Pseudomonas aeruginosa biofilm* bacteria by a halogenated furanone compound. Microbiology **148:**87–102.
23. **Koch B, Nielsen TH, Sørensen D, Andersen JB, Christophersen C, Molin S, Givskov M, Sørensen J, Nybroe O**. 2002. Lipopeptide production in *Pseudomonas* sp. strain dss73 is regulated by components of sugar beet seed exudate via the Gac two-component regulatory system. Appl Environ Microbiol **68:**4509–4516. http://dx.doi.org/10.1128/AEM.68.9.4509-4516.2002.
24. **De Bruijn I, Raaijmakers JM**. 2009. Regulation of cyclic lipopeptide biosynthesis in *Pseudomonas fluorescens* by the ClpP protease. J Bacteriol **191:**1910–1923. http://dx.doi.org/10.1128/JB.01558-08.
25. **Koumoutsi A, Chen XH, Henne A, Liesegang H, Hitzeroth G, Franke P, Vater J, Borriss R**. 2004. Structural and functional characterization of gene clusters directing nonribosomal synthesis of bioactive cyclic lipopeptides in *Bacillus amyloliquefaciens* strain FZB42. J Bacteriol **186:**1084–1096. http://dx.doi.org/10.1128/JB.186.4.1084-1096.2004.
26. **Dennis JJ, Zylstra GJ**. 1998. Plasposons: modular self-cloning minitransposon derivatives for rapid genetic analysis of gram-negative bacterial genomes. Appl Environ Microbiol **64:**2710–2715.
27. **Trieu-Cuot P, Derlot E, Courvalin P**. 1993. Enhanced conjugative transfer of plasmid DNA from *Escherichia coli* to *Staphylococcus aureus* and *Listeria monocytogenes*. FEMS Microbiol Lett **109:**19–24. http://dx.doi.org/10.1111/j.1574-6968.1993.tb06137.x.
28. **Schweizer HP, Hoang TT**. 1995. An improved system for gene replacement and xylE fusion analysis in *Pseudomonas aeruginosa*. Gene **158:**15–22. http://dx.doi.org/10.1016/0378-1119(95)00055-B.
29. **Koch B, Jensen LE, Nybroe O**. 2001. A panel of Tn7-based vectors for insertion of the gfp marker gene or for delivery of cloned DNA into gram-negative bacteria at a neutral chromosomal site. J Microbiol Methods **45:**187–195. http://dx.doi.org/10.1016/S0167-7012(01)00246-9.
30. **Choi KH, Kumar A, Schweizer HP**. 2006. A 10-min method for preparation of highly electrocompetent *Pseudomonas aeruginosa* cells: application for DNA fragment transfer between chromosomes and plasmid transformation. J Microbiol Methods **64:**391–397. http://dx.doi.org/10.1016/j.mimet.2005.06.001.
31. **Whipps JM**. 1987. Effect of media on growth and interactions between a range of soil-borne glasshouse pathogens and antagonistic fungi. New Phytol **107:**127–142. http://dx.doi.org/10.1111/j.1469-8137.1987.tb04887.x.
32. **Gonzalez DJ, Haste NM, Hollands A, Fleming TC, Hamby M, Pogliano K, Nizet V, Dorrestein PC**. 2011. Microbial competition between *Bacillus subtilis* and *Staphylococcus aureus* monitored by imaging mass spectrometry. Microbiology **157:**2485–2492. http://dx.doi.org/10.1099/mic.0.048736-0.
33. **R Development Core Team**. 2009. R: a language and environment for statistical computing. R Foundation for Statistical Computing, Vienna, Austria.
34. **Sambrook J, Russel DW**. 2001. Molecular cloning: a laboratory manual, 3rd ed. Cold Spring Harbor Laboratory, Cold Spring Harbor, NY.